

Original Article

Mammalian Cochlear Hair Cell Imaging Using Optical Coherence Tomography (OCT): A Preliminary Study

Sung-Won Choi , Jieun Kang , Seokhwan Lee , Se-Joon Oh , Hongki Kim , Soo-Keun Kong 

Department of Otorhinolaryngology and Pusan National University School of Medicine, Biomedical Research Institute, Pusan National University Hospital, Busan, Republic of Korea (SWC, JK, SL, SJO, SKK)
Koh Young Technology Inc., Geumcheon-gu, Seoul, Republic of Korea (HK)

Cite this article as: Choi SW, Kang J, Lee S, Oh SJ, Kim H, Kong SK. Mammalian Cochlear Hair Cell Imaging Using Optical Coherence Tomography (OCT): A Preliminary Study. J Int Adv Otol 2021; 17(1): 46-51.

OBJECTIVES: This study aimed to investigate the feasibility of using optical coherence tomography (OCT) to provide information about cochlear microanatomy at a cellular level, specifically of cochlear hair cells in mammals.

MATERIALS AND METHODS: A total of 10 Sprague-Dawley rats were divided into 2 experimental groups for comparing the arrangement of normal and damaged hair cells. Postnatal day 3 Sprague-Dawley rats were used to test the swept-source OCT system, and the images recorded were compared with fluorescence microscope images.

RESULTS: Intracochlear structures (the inner hair cells, outer hair cells, and auditory nerve fibers) were clearly visualized at the individual cellular level.

CONCLUSION: These images reflect the ability of OCT to provide images of the inner hair cells, outer hair cells, and auditory nerve fibers (*ex vivo*). OCT is a promising technology, and these findings could be used to encourage research in the area of cochlear microstructure imaging in the future.

KEYWORDS: Tomography, optical coherence, cochlea, hair cells, auditory, inner, hair cells, auditory, outer

INTRODUCTION

Hearing loss is the most common sensory deficit worldwide ^[1]. In a majority of patients with sensorineural hearing loss, it is irreversible; and there is a limited understanding of the related cochlear pathology ^[2]. A significant obstacle to diagnose pathology of the inner ear is the difficulty to perform noninvasive imaging at sufficient resolution. We commonly use high-resolution computed tomography (CT) and magnetic resonance imaging (MRI) clinically to diagnose inner ear diseases. However, the diameter of cochlea is about 1 cm, and the diameter of the hair cells are in the order of 10 to 50 μm thickness in a human ^[3]. As a consequence, these modalities that are severely limited in spatial resolution to approximately 0.5–1 mm, can only identify gross abnormalities such as a malformation of the cochlea rather than intracochlear defects such as damaged hair cells. Recently, micro-CT and synchrotron radiation-phase contrast imaging (SR-PCI), which have higher spatial resolution (down to 20 μm per voxel) than conventional CT, have also been used to study the cochlear microstructure ^[4,5]. However, only small specimens such as excised tissue can be imaged. The samples are also exposed to high doses of radiation that damage tissues both *in vivo* and *ex vivo*. Immunohistochemical staining (IHC) permit specificity of the particular structures examined using the dye or antibody by allowing specific tagging of a particular protein, or even a pathology. However, this technique requires both sample preparation and imaging and are very time consuming and essentially performed postmortem.

Hearing research in animals has similar limitations as in structural pathology. Better technologies in cochlear hair cell imaging are needed to visualize at the cellular level with higher resolution. In this study, we apply the optical coherence tomography (OCT) technique to solve this problem.

Recently, OCT, a relatively new medical diagnostic imaging modality, provides noninvasive two or three-dimensional cross-sectional images of internal structures with a spatial resolution of 10 to 15 μm in the axial plane and 30 to 40 μm in the transverse plane which is higher than that of CT and MRI ^[6]. OCT is an evolving imaging modality similar to ultrasound imaging, with the exception that light from low-coherence sources, rather than sound, is used to create cross-sectional images of tissues ^[7]. OCT is an imaging technique that has already been established in ophthalmology where it is used to image the retina and cornea ^[8].

This work was presented as a Politzer Prize Session at the 32nd Politzer Society Meeting, 2019, Warsaw, Poland.

Corresponding Address: Soo-Keun Kong E-mail: entkong@gmail.com

Submitted: 03.27.2020 • Revision Received: 10.19.2020 • Accepted: 10.21.2020

Available online at www.advancedotology.org



Content of this journal is licensed under a
Creative Commons Attribution-NonCommercial
4.0 International License.

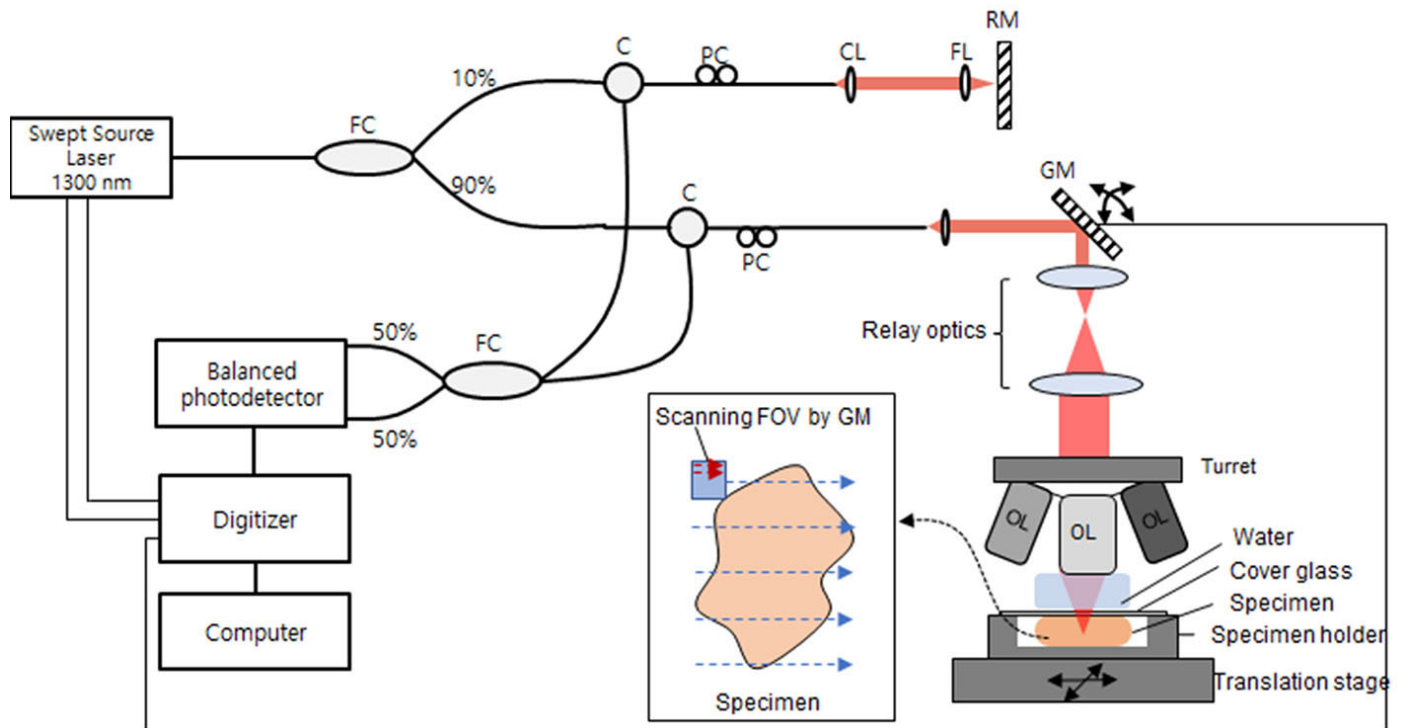


Figure 1. Schematic diagram of the real-time swept-source optical coherence tomography (SS-OCT) system.

FC: fiber coupler; CL: collimation lens; GM: Galvanometer; RM: reference mirror; FL: focusing lens; OL: objective lens; PC: polarization controller; C: circulator.

⁹¹. In the field of cardiology, OCT is also investigated to obtain coronary intravascular images ^[10,11]. In the field of otology, OCT has been used to observe the intracochlear morphology and mechanics in animal models ^[12-17] has enabled the identification of larger structures, including the Reissner's ^[3, 12-16], basilar ^[3, 12-16], and tectorial membranes ^[3, 14-16], the spiral ligament ^[14,16], the 3 scalae of the cochlea ^[12, 14-16], region of sensory epithelium ^[3, 14,15], and the tunnel of Corti ^[3,16]. However, owing to the resolution threshold of OCT, these studies are limited similarly to conventional imaging methodology and are unable to demonstrate visualization of smaller anatomical features, including the inner hair cells (IHC), outer hair cells (OHC), and auditory nerve fibers. Visualization of these smaller auditory structures could be of aid in attaining major therapeutic goals in the treatment of hearing loss. Thus, the objective of this study was to investigate whether OCT was able to resolve cochlear anatomy at a cellular level, especially in mammals.

MAIN POINTS

- OCT enables the assessment of the cochlear microanatomy with better resolution and speed than conventional CT and MRI.
- Intracochlear structures were clearly visualized at individual cellular level using OCT imaging systems.
- In the future, OCT may provide scientists and clinicians a solution for in vivo imaging of human cochlear hair cells.

MATERIALS AND METHODS

Animals

The Sprague-Dawley rat is a well-studied animal model that is commonly used in translational research studies on hearing and hearing loss because its frequency sensitivity and susceptibility to ototoxic medications are similar to that in humans, and its entire cochlea is surgically accessible ^[7]. The Institutional Animal Care and Use Committee (IACUC) of our hospital approved all experimental protocols for this study, and all procedures were carried out in accordance with approved institutional guidelines of the IACUC (PNUH-2017-104). The study was also approved by the Research Animal Care Committee of Laboratory Animals of our University. Postnatal day 3 Sprague-Dawley rats were used. A total of 10 Sprague-Dawley rats were divided into 2 experimental groups: normal and neomycin treated (control) groups.

OCT System and Instrumentation

Figure 1 depicts a schematic of the multi-resolution OCT system built in-house. The light source had a sweep rate of 100 kHz and sweep bandwidth of 100 nm centered at 1,310 nm, corresponding to an axial resolution of 15 μm in air, corresponding to 11.3 μm in tissue. The light coming from the source divides at the fiber coupler: one goes to the reference mirror (10% of the light) and the other goes to the tissue sample (90% of the light). The 2 reflected beams through each circulator combine and interfere at the fiber coupler. The balanced photodiode detector (PDB 470C, Thorlabs, USA) converts the interfered light into an analog electrical signal, and then digitized by DAQ (APX-5050, AVALDATA, JAPAN). The sensitivity of the system was measured to be 103 dB.



Figure 2. Schematic diagram of the experimental timeline. SD: Sprague-Dawley; OCT: optical coherence tomography.

OCT imaging was conducted by scanning 2-axis galvo mirror (GVS012, Thorlabs, USA), and wide-field OCT images were generated by stitching and reconstructing the multiple field of view (FOV) images acquired by moving 2-axis translation stages. Transverse resolutions were measured to be 1.55 μm and 7.81 μm using interchangeable Olympus 20 \times water immersion objective (XLUMPLLN 20XW, NA=1.0) and Thorlabs 5 \times objective (5 \times , NA=0.036). FOV of 20 \times objective was measured to be 0.8 mm \times 0.8 mm. FOV of 5 \times objective was measured to be 4 mm \times 4 mm, respectively. Objective were changed by built in-house turret automatically. Variable beam expander was designed and adapted to provide variable collimation beam size by changing objective. Dispersion from different objectives was compensated numerically.

OCT Imaging and Image Analysis

Two-dimensional color images of the tissue surface were captured through Nikon 1 \times objective (Plan Achromat Infinity, NA = 0.04, 20 mm² FOV) to designate the region of interest for OCT imaging. OCT imaging was performed at the selected region from 2D color images because spatial coordinates between 2D color image and OCT image were calibrated formerly. In addition, spatial coordinates between translation stages and OCT image were calibrated to generate wide-field OCT images. Wide field of view images were created by stitching and reconstructing the multiple FOV images acquired by moving the translation stages. During OCT imaging, specimens were removed from PBS and positioned beneath the OCT laser aperture in a dry specimen holder. Specimens were adjusted in a 3-axis direction to achieve optical focus. SmartFinder (Koh Young Technology, South Korea), a software program built-in-house, was used to reconstruct multiplanar OCT images, generate rotations, enlarge images, and establish image opacity.

Specimen Preparation

Figure 2 depicts a schematic diagram of the experimental timeline. Postnatal day 3 Sprague-Dawley rats were decapitated on ice, and the temporal bone was harvested in 50 unit/mL of penicillin (P3032, Sigma Aldrich, USA) containing Dulbecco's phosphate-buffered saline solution (14190, Gibco, USA), aseptically. To expose the cochlea, tympanic bulla and excess tissue were removed from the temporal bone region. The exposed lateral cochlear capsule was peeled off gently, and the membranous labyrinth was visualized. The spiral ligament and stria vascularis were removed to separate the organ of Corti [17-19]. Extracted explant was moved to a prepared, saline coated slide glass (5116-20F, Muto Pure Chemicals, Japan) which had 0.2 mm of polydimethylsiloxane (Sylgard 184, SeWang Hitech, Korea) wall with a growth medium: high glucose, Dulbecco's modified Eagle's medium (11995065, Life Technologies, USA) with 10% of fetal

bovine serum (16000044, Gibco, USA) and 50 unit/mL of penicillin (P3032, Sigma Aldrich, USA). In the group with hair cell damage, the explants were treated with 0.65 mg/mL final concentration of neomycin, which is an ototoxic antibiotic, for 6 hours. The explants were then rinsed several times by phosphate-buffered saline (PBS) solution to remove any remaining traces of neomycin and treated with fresh media. The cover glass was then put on the cochlear explants. Next, PBS-solution was dropped on the slide glass, and the OCT video was recorded.

After the OCT image was recorded, the media was changed again, and the explants were incubated overnight in a humidified atmosphere containing 5% carbon dioxide. After the explant was attached to the saline coated slide, the medium was replaced by 4% paraformaldehyde (P2031, Biosesang, Korea) to fix the tissue for 1 hour. Following the rinsing of the explant with PBS several times, it was permeabilized with 0.3% TritonX-100 (T9284, Sigma Aldrich, USA) in PBS for 60 minutes at room temperature and stained with Alexa Fluor 488-conjugated phalloidin (1:300; A12379, Life Technologies, USA) for 60 minutes. Phalloidin conjugates are used to visualize the hair cell by labeling the actin filament (F-actin) of stereocilia in cochlear hair cells and used to distinguish the hair cell from the explanted organ of Corti [20]. Alexa 488 phalloidin visualizes the hair cells through the green colored stereocilia bundle. All images were viewed with a fluorescent microscope (Eclipse 80i, Nikon, Tokyo, Japan). This microscope was set the 20 \times objective lens (MRH00201, Nikon, Tokyo, Japan) which has 0.50 of objective numerical aperture (NA) and blue excitation filter (B-2A, Nikon, Tokyo, Japan) excited from 450 nm to 490 nm.

To confirm the nerve cell viability, MTT assay was performed using inner ear cells, including auditory nerve cell. Auditory nerve cells were extracted from a 3-day old rat and isolated with 25 mg/mL collagenase (17101015, Thermo Fisher) and trypsin (25200056, Gibco, USA) dispersed HBSS solution at 37 $^{\circ}\text{C}$ for 20 minutes. The isolated cells were then seeded in a cell dish coated with poly L-ornithine (P4957, Sigma Aldrich) and 20 $\mu\text{g}/\text{mL}$ of Laminin (23017015, Thermo Fisher) and cultured with DMEM (12430047, Thermo Fisher) media containing 10% FBS (S001-01, Welgene), 1% penicillin-streptomycin (15140163, Thermo Fisher), 1% N_2 supplement (17502048, Thermo Fisher), and 1.5 mg/mL of glucose (G7021, Sigma Adrich). A total of 30,000 cells were seeded in a 24-well cell plate and treated with 0 mg/mL, 0.30 mg/mL, 0.65 mg/mL, and 1.3 mg/mL of neomycin for 24 hours. After incubation, MTT contained media was treated and incubated for 3 hours and exchanged as 10% SDS solution (TLP-103.1, TransLab, Korea). The absorbance was measured at 570 nm. Anti-S100 antibody (MAB079-1, Merck) and anti-160 kD neurofilament medium

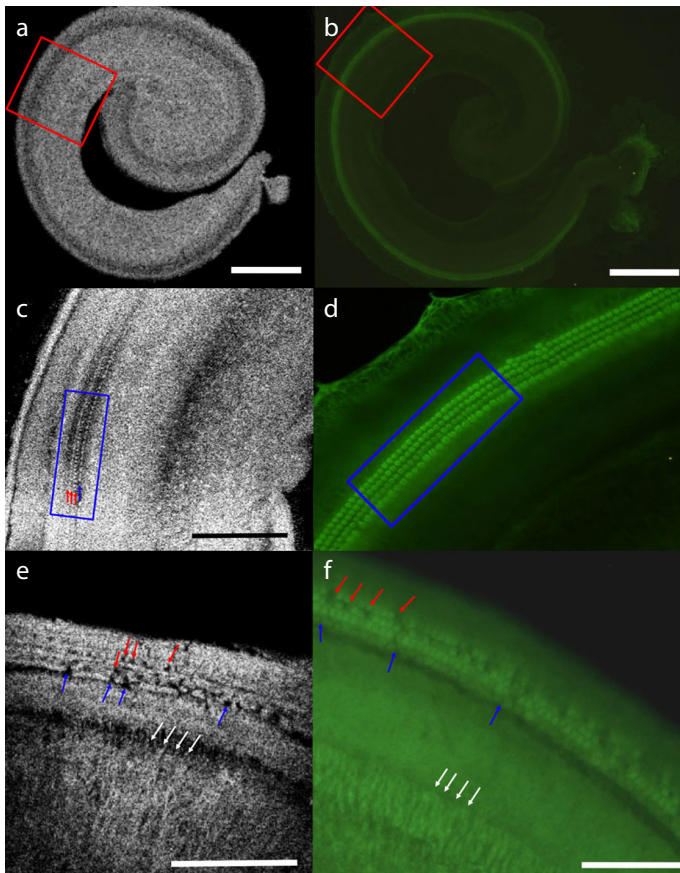


Figure 3. a-f. Optical coherence tomography (OCT) images and fluorescent microscope images of the Sprague-Dawley rat organ of Corti (normal group: A-D, neomycin treated group: E, F). (a) En-face image from swept-source optical coherence tomography (SS-OCT), depicting the full turn of organ of Corti. Scale=500 μm ; imaging depth=50 μm . (b) Fluorescent microscope image corresponding to the orientation presented in (a). Scale=500 μm . (c) Zoomed-in view of the organ of Corti, representing the region boxed in red in (a). The regions of inner hair cells (blue arrow) and 3 rows of outer hair cells (red arrow) were identified. Scale=100 μm . (d) Fluorescent microscope image corresponding to the orientation presented in (c). Scale=100 μm . (e) Partial destruction of cochlear hair cells and alignment were identified. Inner hair cells (blue arrow) and outer hair cells (red arrow) are observed after neomycin treatment. Additionally, auditory nerve fibers are clearly identified with OCT because of their location and radial trajectory (white arrow). Scale=100 μm . (f) Fluorescent microscope image corresponding to the orientation presented in (a). Scale=100 μm .

antibody (ab7794, Abcam) were used for neuron cell staining as a first antibody, and DAPI was used for nuclear staining. Anti-mouse antibody (A32723, Thermo Fisher) was used as the second antibody to detect the first antibody.

RESULTS

The area was exposed from the top, and the extracted organ of Corti was imaged with OCT (Figure 3A). The thickness of the OCT sample was $82.5 \pm 14.10 \mu\text{m}$ measured by OCT and that of the stained sample was $38.0 \pm 4.90 \mu\text{m}$ measured by confocal microscope. OCT permitted imaging in a $0.8 \text{ mm} \times 0.8 \text{ mm}$ FOV. Fluorescent microscopic image of the same sample is shown in Figure 3B. Both images reveal full turns of the extracted organ of Corti. Figures 3C and 3D zoom in on the red boxed region in Figures 4A and 4B, respectively. Figure 3C reveals the region of IHC and 3 rows of OHCs. A higher resolution image of the region is illustrated in Figure 4A, depicting the sensory cells (IHC and

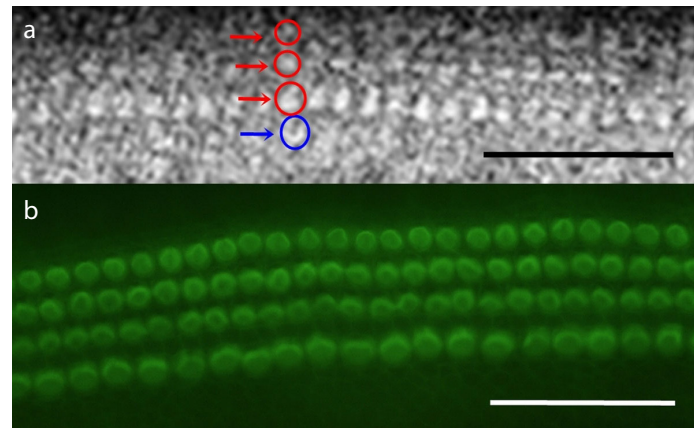


Figure 4. a, b. Optical coherence tomography images and fluorescent microscope images of individual cochlear hair cells. (a) The individual inner hair cells (blue arrow and circle) and three rows of outer hair cells (red arrow and circle) were identified. Scale=50 μm . (b) Fluorescent microscope image, corresponding to the orientation presented in (a). Scale=50 μm .

OHC) of the organ of Corti. The image shows the area where the hair cells are present, and individual IHC and OHC are clearly identified. Figures 3B, 3D, and 4B show fluorescent microscope images of the same sample as recorded with the OCT in the extracted SD rat organ of Corti for orientation.

To confirm that the alignment identified in the OCT images were hair cells, we also imaged a control group that was treated with neomycin, an ototoxic drug that damages hair cells. Figures 3E and 3F show partial destruction of cochlear hair cells and alignment in the same region. From these points of view, the region we identified in the OCT images were confirmed to be cochlear hair cells. In addition, auditory nerve fibers were identified with OCT according to their location and radial trajectory (Figure 3).

Density of the extracted inner ear cells after 24 hours treatment with neomycin had no big difference between either groups (Figures 5A–5D). Even in the MTT assay result, samples treated with neomycin for 24 hours did not decrease the viability of the cells compared with the control (Figure 5).

DISCUSSION

OCT is an imaging technology that creates cross-sectional images by using the interference effect of a low-coherence light source in infrared wavelength reflected back by the tissue structure^[17]. Imaging of the cochlear microstructure is a novel application of OCT. Iyer et al.^[16] reported that high-resolution OCT imaging could resolve the guinea pig cochlea, including hair cells by corresponding the orientation presented in immunohistochemical staining, previously. Unlike previous studies, this is the first study that clearly identified each hair cell, including 3 rows of OHC and 1 row of IHC, on OCT in mammalian cochlea to the best of our knowledge. We identified auditory nerve fibers in both OCT and fluorescent microscope images; these are well known to degenerate after the hair cell damage on overexposure to ototoxic drugs in mammalian, received short term treatment to visualize the serious damage^[18]. As a result of MTT assay *in vitro* experiment, samples treated with neomycin for 24 hours did not decrease the viability of the cells compared with the control (Figure 5). Spiral ganglion neurons (SGNs) are bipolar neurons, and

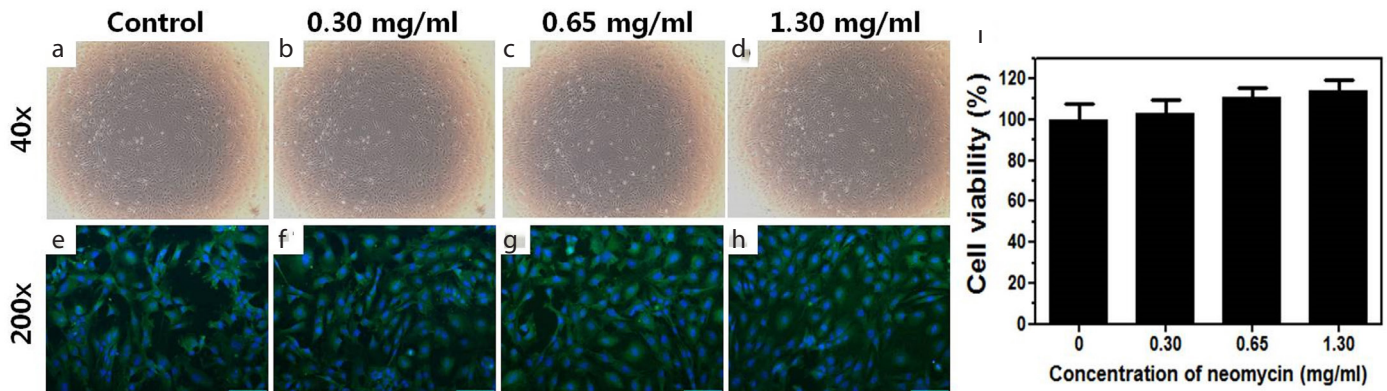


Figure 5. a-i. *In vitro* cell viability experiment using primary inner ear cells with neomycin. (a-d) Density of the extracted inner ear cells after 24 hours treatment of neomycin. (e-h) Distribution of living neuron cells by anti-S100 and anti-160 kD neurofilament antibody as the green color after 24 hours treatment of neomycin. Scale=100 μ m. (i) Cell viability after 24-hour treatment with neomycin.

their survival is influenced by many factors. Among them, hair cells provide survival promoting stimuli; neurotrophic factors and primary excitatory input causing depolarization of SGNs [19]. Hence, hair cell is important for the survival of SGNs, but it is well known that aminoglycoside antibiotics like neomycin cause hair cell death. After hair cell loss, SGNs degenerate because the ganglia are not innervated by the hair cell [20]. In this experiment, 24-hour treatment of neomycin was not enough to induce the serious auditory nerve degeneration, even in high concentration, 1.3 mg/mL.

The clinical applications of OCT in the human cochlea face significant technical barriers. Bone density and bone thickness remain challenges to improve depth penetration [13]. A major obstacle for employing OCT in human intracochlear imaging is the penetration depth of the incident light, which for a 1,310 nm light source is approx. 1.25 mm on average [11]. However, it can be applied in animal research more immediately. There are advantages to using OCT over other conventional imaging tools. Various modalities have been used for imaging the cochlea. Current studies using animal models for hearing impairments commonly use techniques such as confocal and 2-photon microscopy, in parallel with histology and immunohistochemistry, to detect and visualize changes in cochlear morphology. These techniques require both sample preparation and imaging and are very time consuming and are essentially performed postmortem. Recently, micro-CT and SR-PCI, which have a higher spatial resolution (down to 20 μ m per voxel) than conventional CT, have also been used to study the cochlear microstructure [4,5]. Micro-CT images suffer from problems such as artifacts, noise, low contrast resolution, and restrictions on specimen size [21,22]. These problems limit the ability to visualize the cochlear microanatomy without using histological sections as a reference [23]. The use of SR-PCI can potentially overcome these shortcomings, making cochlear inner structures visible [24-26]. However, staining and dehydration of the specimens was required to improve the visualization of soft tissues [25]. It has been reported that staining specimens causes distortion and shrinkage of the cochlear microstructure because of dehydration [26]. In addition, the samples are exposed to high doses of radiation that damage tissues both *in vivo* and *ex vivo*.

Recently, various studies have attempted to apply OCT systems in the field of otology. OCT provided noninvasive, nondestructive, 2D

cross-sectional, and 3D volumetric images of the middle-ear and inner ear structures in rodents [27]. Anatomical depth-resolved imaging has shown promising potential for morphological measurements of the middle and inner ear in chinchillas and mice with blast trauma [28,29]. Moreover, OCT has demonstrated its capability as a functional analytical tool by characterizing the vibration of middle and inner ear structures using the Doppler principle without contrast labeling to identify fluid, cellular structures, and bone [30].

In this study, we identified the microstructure of the cochlea immediately after dissecting the specimen. Therefore, using these OCT techniques, the time required for observing the IHC and OHC is drastically reduced compared with conventional imaging modalities.

Although microanatomic structures within cochlea were clearly identified in this study, there were certain limitations. In this study, OCT images were applied postmortem, and the specimens used were excised and dissected to facilitate manipulation. Nonetheless, these findings imply an important and progressive step forward in the ability of OCT to identify the mammalian cochlea at a cellular level. This research can help improve the OCT technology and enable it to be used for a wider range of applications in the future.

CONCLUSION

Currently, there are no readily available imaging modalities that can provide tomographic information on cochlear microstructure without biopsy and fixation. To understand the link between inner ear pathology and auditory function, it is essential to develop a new imaging system that can explain the anatomical structure of the inner ear. OCT is an imaging modality that enables the assessment of the cochlear microanatomy with a resolution and speed that is superior to conventional CT and MRI. This study demonstrates the preliminary results of using OCT imaging systems for determining cochlear microanatomy such as IHC, OHC, and auditory nerve fibers (*ex vivo*); however, significant progress is still needed. Future efforts should aim to determine whether it is possible to generate similar imaging results in live animal subjects. Although several technical problems remain, OCT may provide scientists and clinicians a solution for *in vivo* human cochlear hair cell imaging. Our findings could be used to encourage research into the area of cochlear microstructure imaging in the future.

Ethics Committee Approval: This study was approved by the institutional guidelines of the Institutional Animal Care and Use Committee (IACUC) of Pusan National University Hospital (PNUH-2017-104).

Informed Consent: N/A

Peer-review: Externally peer-reviewed.

Author Contributions: Concept – C.S.W.; Design – C.S.W., K.S.K.; Supervision – K.J.; Resource – K.H., L.S.; Materials – K.J., O.S.J.; Data Collection and/or Processing – C.S.W., K.J.; Analysis and/or Interpretation – K.J., L.S.; Literature Search – C.S.W., O.S.J.; Writing – C.S.W.; Critical Reviews – K.S.K.

Acknowledgements: The authors would like to thank Minkyu Kim and Jeonghun Choi for useful discussions and a helping hand.

Conflict of Interest: The authors have no conflict of interest to declare.

Financial Disclosure: This work was supported by a Basic Science Research Program grant (NRF-2018R1D1A1B07048778) from the National Research Foundation of Korea. This work was supported by clinical research grant from Pusan National University Hospital in 2020.

REFERENCES

- Oishi N, Schacht J. Emerging treatments for noise-induced hearing loss. *Expert Opin Emerg Drugs* 2011; 16: 235-45. [Crossref]
- Landegger LD, Psaltis D, Stankovic KM. Human audiometric thresholds do not predict specific cellular damage in the inner ear. *Hear Res* 2016; 335: 83-93. [Crossref]
- Gao SS, Xia A, Yuan T, Raphael PD, Shelton RL, Applegate BE, et al. Quantitative imaging of cochlear soft tissues in wild-type and hearing-impaired transgenic mice by spectral domain optical coherence tomography. *Optic Express* 2011; 19: 15415-28. [Crossref]
- Bellos C, Rigas G, Spiridon IF, Bibas A, Iliopoulou D, Böhnke F, et al. Reconstruction of cochlea based on micro-CT and histological images of the human inner ear. *BioMed Res Int* 2014; 2014: 485783. [Crossref]
- Elfarnawany M, Riyahi Alam S, Rohani SA, Zhu N, Agrawal SK, Ladak HM. Micro-CT versus synchrotron radiation phase contrast imaging of human cochlea. *J Microsc* 2017; 265: 349-57. [Crossref]
- Cho NH, Jang JH, Jung W, Kim J. In vivo imaging of middle-ear and inner-ear microstructures of a mouse guided by SD-OCT combined with a surgical microscope. *Optic Express* 2014; 22: 8985-95. [Crossref]
- Huang D, Swanson EA, Lin CP, Schuman JS, Stinson WG, Chang W, et al. Optical Coherence Tomography. *Science* 1991; 254: 1178-81. [Crossref]
- Spaide RF, Koizumi H, Pozzoni MC. Enhanced depth imaging spectral-domain optical coherence tomography. *Am J Ophthalmol* 2008; 146: 496-500. [Crossref]
- Shah SU, Kaliki S, Shields CL, Ferenczy SR, Harmon SA, Shields JA. Enhanced depth imaging optical coherence tomography of choroidal nevi in 104 cases. *Ophthalmology* 2012; 119: 1066-72. [Crossref]
- Jang IK, Tearney GJ, MacNeill B, Takano M, Moselewski F, Iftima N, et al. In vivo characterization of coronary atherosclerotic plaque by use of optical coherence tomography. *Circulation* 2005; 111: 1551-5. [Crossref]
- Grube E, Gerckens U, Buellfeld L, Fitzgerald PJ. Images in cardiovascular medicine. Intracoronary imaging with optical coherence tomography: a new high-resolution technology providing striking visualization in the coronary artery. *Circulation* 2002; 106: 2409-10. [Crossref]
- Wong BJ, de Boer JF, Park BH, Chen Z, Nelson JS. Optical coherence tomography of the rat cochlea. *J Biomed Opt* 2000; 5: 367-70. [Crossref]
- Wong BJ, Zhao Y, Yamaguchi M, Nassif N, Chen Z, De Boer JF. Imaging the internal structure of the rat cochlea using optical coherence tomography at 0.827 microm and 1.3 microm. *Otolaryngol Head Neck Surg* 2004; 130: 334-8. [Crossref]
- Lin J, Staecker H, Jafri MS. Optical coherence tomography imaging of the inner ear: a feasibility study with implications for cochlear implantation. *Ann Otol Rhinol Laryngol* 2008; 117: 341-6. [Crossref]
- Subhash HM, Davila V, Sun H, Nguyen-Huynh AT, Nuttall AL, Wang RK. Volumetric in vivo imaging of intracochlear microstructures in mice by high-speed spectral domain optical coherence tomography. *J Biomed Opt* 2010; 15: 036024. [Crossref]
- Iyer JS, Batts SA, Chu KK, Sahin MI, Leung HM, Tearney GJ, et al. Micro-optical coherence tomography of the mammalian cochlea. *Sci Rep* 2016; 16: 33288. [Crossref]
- Zhou H, Ma X, Liu Y, Dong L, Luo Y, Zhu G, et al. Linear polyethyleneimine-plasmid DNA nanoparticles are ototoxic to the cultured sensory epithelium of neonatal mice. *Mol Med Rep* 2015; 11: 4381-8. [Crossref]
- Leake PA, Hradek GT. Cochlear pathology of long term neomycin induced deafness in cats. *Hear Res* 1988; 33: 11-33. [Crossref]
- Alam SA, Robinson BK, Huang J, Green SH. Prosurvival and proapoptotic intracellular signaling in rat spiral ganglion neurons in vivo after the loss of hair cells. *J Comp Neurol* 2007; 503: 832-52. [Crossref]
- Schacht J, Talaska AE, Rybak LP. Cisplatin and aminoglycoside antibiotics: hearing loss and its prevention. *Anat Rec (Hoboken)* 2012; 295: 1837-50. [Crossref]
- Shibata T, Matsumoto S, Agishi T, Nagano T. Visualization of Reissner membrane and the spiral ganglion in human fetal cochlea by micro-computed tomography. *Am J Otolaryngol* 2009; 30: 112-20. [Crossref]
- Noble JH, Labadie RF, Gifford RH, Dawant BM. Image-guidance enables new methods for customizing cochlear implant stimulation strategies. *IEEE Trans Neural Syst Rehabil Eng* 2013; 21: 820-9 [Crossref]
- Teymouri J, Hullar T, Holden TA, Chole RA. Verification of computed tomographic estimates of cochlear implant array position: a micro-CT and histological analysis. *Otol Neurotol* 2011; 32: 980-6. [Crossref]
- Lareida A, Beckmann F, Schrott-Fischer A, Gluekert R, Freysinger W, Müller B. High-resolution X-ray tomography of the human inner ear: synchrotron radiation-based study of nerve fibre bundles, membranes and ganglion cells. *J Microsc* 2009; 234: 95-102. [Crossref]
- Rau C, Hwang M, Lee WK, Richter CP. Quantitative X-ray tomography of the mouse cochlea. *PLoS One* 2012; 7: e33568. [Crossref]
- Richter CP, Shintani-Smith S, Fishman A, David C, Robinson I, Rau C. Imaging of cochlear tissue with a grating interferometer and hard X-rays. *Microsc Res Tech* 2009; 72: 902-7 [Crossref]
- Oh SJ, Lee IW, Wang SG, Kong SK, Kim HK, Goh EK. Extratympanic observation of middle and inner ear structures in rodents using optical coherence tomography. *Clin Exp Otorhinolaryngol* 2020; 13: 106-12. [Crossref]
- Ramier A, Cheng JT, Ravicz ME, Rosowski JJ, Yun SH. Mapping the phase and amplitude of ossicular chain motion using sound-synchronous optical coherence vibrometry. *Biomed Opt Express* 2018; 9: 5489-502. [Crossref]
- Kim J, Xia A, Grillet N, Applegate BE, Oghalai JS. Osmotic stabilization prevents cochlear synaptopathy after blast trauma. *Proc Natl Acad Sci U S A* 2018; 115: E4853-60. [Crossref]
- Cooper NP, Vavakou A, van der Heijden M. Vibration hotspots reveal longitudinal funneling of sound-evoked motion in the mammalian cochlea. *Nat Commun* 2018; 9: 3054. [Crossref]